

# Unified Path Planner with Adaptive Safety and Optimality

Jatin Kumar Arora, Soutrik Bandyopadhyay and Shubhendu Bhasin

**Abstract**—Path planning for autonomous robots presents a fundamental trade-off between optimality and safety. While conventional algorithms typically prioritize one of these objectives, we introduce the Unified Path Planner (UPP), a unified framework that simultaneously addresses both. UPP is a graph-search-based algorithm that employs a modified heuristic function incorporating a dynamic safety cost, enabling an adaptive balance between path length and obstacle clearance. We establish theoretical sub-optimality bounds for the planner and demonstrate that its safety-to-optimality ratio can be tuned via adjustable parameters, with a trade-off in computational complexity. Extensive simulations show that UPP achieves a high success rate, generating near-optimal paths with only a negligible increase in cost over traditional A\*, while ensuring safety margins that closely approach those of the classical Voronoi planner. Finally, the practical efficacy of UPP is validated through a hardware implementation on a TurtleBot, confirming its ability to navigate cluttered environments by generating safe, sub-optimal paths.

## I. INTRODUCTION

The increasing integration of robots into complex human environments has made robust and efficient path planning a cornerstone of modern robotics. To ensure smooth, safe, and productive operation—from autonomous vehicles [1]–[3] and UAVs [4] to robotic arms [5]–[8] and warehouse automation systems [9], [10]—robots must navigate dynamic and cluttered spaces effectively. This necessity has spurred the development of diverse path-planning methodologies, each with its own strengths and limitations.

The literature on path planning is extensive, with major families of algorithms offering different approaches to the problem. Grid-based search algorithms, such as A\* [11], form a foundational category. Innovations in this area include modifications to accelerate search time at the cost of optimality [12] and techniques for planning over continuous grid edges to produce shorter paths [13]. For dynamic environments, replanning algorithms like D\* [14] have been developed to efficiently update paths without recalculating from scratch. Sampling-based algorithms like the Rapidly-exploring Random Tree (RRT) [15] have revolutionized planning in high-dimensional configuration spaces. Subsequent variants, such as RRT-Smart [16], introduced intelligent sampling and path optimization to improve convergence and cost, while FAST-RRT [17] significantly reduced execution time through advanced sampling and steering strategies. Combinatorial methods [18]–[20], such as those using Voronoi diagrams [20], focus on maximizing path safety by maintaining the largest possible distance from obstacles. Furthermore, potential field-based methods [21]–[23] draw inspiration from physics, using attractive and repulsive forces to guide the robot. Modified versions of these algorithms

have successfully addressed classic problems like local minima avoidance.

While these algorithms excel at either optimizing for the shortest path (like A\* and its variants) or maximizing safety (like Voronoi-based planners), a critical research gap exists for frameworks that can jointly and adaptively manage both objectives. Recent research has made significant strides toward bridging this gap. Chu et al. [24] proposed Optimized-A\* that introduced an obstacle raster coefficient and a turning function to improve trajectory safety. However, this method addresses obstacle avoidance in more absolute terms and offers limited control over the specific safety distance between nodes. Control Barrier Functions (CBFs) have been integrated into planners like CBF-RRT [25] to enforce safety-critical constraints, demonstrating superior performance over other RRT-based methods in generating safe paths. SDF-A\* [26] leverages a Signed Distance Function (SDF) to embed safety information directly into the planning process, showing significant improvements in both safety and exploration compared to traditional algorithms. Despite these advancements, existing solutions that address both objectives often come with significant drawbacks. They can incur high computational complexity, force a large trade-off that excessively penalizes path cost for minor gains in safety, or rely on fixed, non-tunable safety margins that cannot adapt to changing operational needs.

To overcome these gaps, we propose the Unified Path Planner (UPP), a framework designed to jointly and efficiently optimize for both optimality and safety through a flexible and adaptive heuristic. Our contributions are three-fold:

- 1) We introduce a unified and adaptive heuristic function that allows for a tunable trade-off between optimality and safety to meet specific application requirements.
- 2) We provide extensive simulation results and hardware experiments across diverse environments, comparing UPP against a suite of both traditional and state-of-the-art safe-optimal planning algorithms.
- 3) We establish theoretical sub-optimality bounds on the path cost generated by UPP, providing a formal guarantee of its performance.

## II. PROBLEM DEFINITION

The objective is to find a collision-free, optimal, and safe path for an autonomous mobile robot navigating from an initial configuration to a goal configuration within a static, two-dimensional workspace. A key requirement of the path is to maintain a maximum possible distance from obstacles

while minimizing its total length. The problem is formulated as follows:

- 1) A world  $W$  which is represented as a continuous space  $W \subseteq \mathbb{R}^2$ .
- 2) An obstacle region  $O$ , is a subset of the World  $O \subset W$ .
- 3) A rigid robot  $A$  defined in  $W$ .
- 4) The configuration space,  $C$ , is the set of all possible poses (translations and rotations) of the robot  $A$ .
- 5) The free configuration space,  $C_{\text{free}}$ , and the obstacle configuration space,  $C_{\text{obs}}$ , are derived from  $C$ .
- 6) Given an initial configuration  $p_I \in C_{\text{free}}$  and final goal configuration  $p_G \in C_{\text{free}}$ , the task is to find a path  $J(s) : [0, 1] \rightarrow C_{\text{free}}$  that is collision-free and minimizes a combined cost function incorporating both path length and safety.

### III. PROPOSED METHODOLOGY

We introduce the Unified Path Planner (UPP), a graph-based search algorithm, inspired by the  $A^*$ , that uses a novel heuristic function to dynamically integrate both optimality and safety costs. The core assumption is that the robot can identify obstacles within a specific sensing radius,  $R$ .

#### A. Heuristic Function

The total cost of a path from the start node to a given node  $n$ , and then to the goal, is defined by the function  $f(n)$ :

$$f(n) = g(n) + h(n), \quad (1)$$

where:

- $f(n)$ : total heuristic cost,
- $g(n)$ : cost to reach node  $n$  from the start,
- $h(n)$ : estimated cost-to-go, representing the heuristic estimate of the cost from node  $n$  to the goal.

Graph traversal path-finding algorithms use the heuristic  $h(n)$  to estimate the remaining cost from node  $n$  to the goal, guiding the search toward promising paths. The next node to expand is selected based on the minimum total cost  $f(n) = g(n) + h(n)$ , thereby prioritizing nodes that balance the cost so far with the estimated cost-to-go.

The proposed heuristic function,  $h(n)$ , is a weighted combination of three components: an optimality-focused distance (infinity norm and first norm), a safety-focused distance function. The combined heuristics are defined as:

$$h(n) = \alpha h_1(n, g) + (1 - \alpha) h_\infty(n, g) + \beta S(n) \quad (2)$$

where  $h_1(n, g) \triangleq \|n - g\|_1$  denotes the Manhattan distance between the current node and the goal position,  $h_\infty(n, g) \triangleq \|n - g\|_\infty$  denotes the Chebyshev distance between the current node and the goal position, with  $\alpha \in [0, 1]$  and  $\beta \in \mathbb{R}_+$  being the weights. The heuristic  $S(n) : \mathbb{R}^2 \rightarrow \mathbb{R}$  denotes the the safety term defined as follows

$$S(n) \triangleq \sum_{\Delta n \in [-R, R]^2} \frac{\mathbb{I}[n + \Delta n \in \mathcal{O}]}{\|\Delta n\|_\infty + \epsilon}, \quad (3)$$

where  $\mathbb{I}(\cdot)$  represents the indicator function, which takes the value of one when the condition in its argument is true and

the value of zero otherwise. The parameter  $\epsilon \ll 1$  is used to evade singularity in certain edge cases.

While the Manhattan distance metric incentivizes movements along the grid-lines, the Chebyshev metric induces diagonal movements of the path-planning agent. The user-defined weight  $\alpha$  provides a way to tune the desired behavior of the robot depending on the environment that the agent is planning for.

*Remark 1:* The radius  $R$  considered in (3) depicts the grid size of the neighborhood that a robot considers for safety cost calculation to avoid obstacles. It is inspired by the vision-based capabilities of a robot in Radius  $R$ . The cost is inversely proportional to the Chebyshev distance from the obstacle.

The pseudo-algorithm is described in Algorithm 1. Fig. 1 depicts the heuristics representations of the safety function and the combined heuristics.

Before proceeding, we define the admissibility of a heuristic function.

*Definition 1 (Admissible heuristics [27]):* A heuristic  $h : \mathbb{R}^n \rightarrow \mathbb{R}$  is said to be admissible, if  $h(n) \leq h^*(n) \forall n \in W$  where the  $h^*(n)$  denotes the optimal cost obtained from the node  $n$ . In other words, the admissible heuristic function never overestimates the optimal cost.

*Lemma 1 (Suboptimality Bound for UPP):* Let  $\pi_{\text{UPP}}$  be the path returned by the Unified Path Planner (UPP) using the heuristic defined in Equation (2), and let  $\pi^*$  be the optimal path of cost  $J^*$  and step length  $L^*$ . As the heuristic includes a proximity-based penalty term with bounded maximum contribution, so the total cost satisfies:

$$J_{\text{UPP}} \leq J^* + \beta \cdot \frac{(2R + 1)^2}{\epsilon} \cdot L^*.$$

*Proof:* It can be shown that the heuristic  $h_1$  (Section 3.6 [27]) and  $h_\infty$  [28] are admissible. Thus, for every node  $n$  we have

$$h_1(n) \leq h^*(n) \quad \text{and} \quad h_\infty(n) \leq h^*(n).$$

Multiplying these inequalities by the nonnegative scalars  $\alpha$  and  $1 - \alpha$  (where  $0 \leq \alpha \leq 1$ ) gives

$$\alpha h_1(n) \leq \alpha h^*(n), \quad \text{and} \quad (1 - \alpha) h_\infty(n) \leq (1 - \alpha) h^*(n).$$

Adding these inequalities yields

$$\alpha h_1(n) + (1 - \alpha) h_\infty(n) \leq \alpha h^*(n) + (1 - \alpha) h^*(n) = h^*(n).$$

Therefore,  $\alpha h_1 + (1 - \alpha) h_\infty$  is admissible.

$$\alpha h_1(n) + (1 - \alpha) h_\infty(n) \leq h^*(n),$$

where  $h^*(n)$  is the true cost-to-go from  $n$ .

For the safety equation defined in (3), the worst case is that every cell in the neighborhood is an obstacle, and each term is upper bounded by  $1/\epsilon$ . The number of cells in the square neighborhood is  $(2R + 1)^2$ . We can thus write:

$$S(n) \leq \frac{(2R + 1)^2}{\epsilon}.$$

Using [29], we write:

$$h(n) \leq h^*(n) + \beta \frac{(2R+1)^2}{\epsilon},$$

where the path cost of the proposed method is bounded suboptimal.

If the optimal path has the length of  $L^*$ , then UPP returns a path of cost:

$$J_{\text{UPP}} \leq J^* + \beta \cdot \frac{(2R+1)^2}{\epsilon} \cdot L^*. \quad \blacksquare$$

**Remark.** The bound in Lemma 1 characterizes the worst-case performance of UPP. In practice, observed costs are typically much lower, as the bound serves as a formal sub-optimality guarantee rather than an empirical cost estimate, reflecting the trade-off between optimality and safety.

As UPP inherits the computational complexity of A\*, it incurs a multiplicative  $O(R^2)$  overhead per expansion, since the safety evaluation requires inspecting all cells within a radius  $R$ , whose count grows quadratically with  $R$ .

#### IV. SIMULATION

The Unified Path Planner (UPP) generates a sub-optimal and safe path. We have conducted simulations to give a detailed analysis of the working of the algorithm. First, we will show how paths vary with various parameters and in comparison with various other algorithms. These simulations have been conducted on a 13th Gen Intel(R) Core(TM) i7-13650HX 2.60 GHz processor and 16 GB RAM.

##### A. Variation of Alpha

Variable Alpha	Total Turning Angle (Degree)
0	495.23
0.25	630.12
0.5	360.33
0.75	540.35
1	450.14

TABLE I: Metrics for comparison of variable alpha

The  $\alpha$  parameter plays a significant role in balancing the heuristics of Chebyshev and Manhattan distance. If  $0 \leq \alpha \leq 0.5$ , it favors more diagonal movement, as the distance represents more of the infinity norm distance, which leads to L-shaped movements. If  $0.5 \leq \alpha \leq 1$ , it favors more of the 1st norm or Manhattan distance, which leads to more grid-based movements. If  $\alpha = 0.5$ , it creates a balance between the turning angle and equivalent movements in terms of turning angle. Table 1 and Fig. 2 represent the effect of alpha on the path in metrics and visualization, respectively. It can be observed that the minimum turning angle is when  $\alpha = 0.5$ , i.e.,  $360.33^\circ$ .

---

#### Algorithm 1 Unified Path Planner (UPP)

---

**Require:** Grid map  $G$ , start  $s$ , goal  $g$ , parameters  $\alpha, \beta, R$   
**Ensure:** Optimal and safe path  $P$  from  $s$  to  $g$  or FAILURE

- 1:  $O \leftarrow$  empty min-heap (priority queue ordered by  $f$ )
- 2:  $CameFrom \leftarrow \emptyset$ ,  $Visited \leftarrow \emptyset$
- 3: Initialize  $gCost(x) \leftarrow +\infty$  for all  $x \in G$ ;
- 4:  $f(s) \leftarrow gCost(s) + \text{COMBH}(s, g, G, \alpha, \beta, r)$
- 5: Push  $\langle f(s), s, (0, 0) \rangle$  into  $O$   $\triangleright$  store  $(f, \text{node}, \text{prevMove})$
- 6: **while**  $O$  not empty **do**
- 7:   Pop  $\langle f_{\text{curr}}, \text{curr}, \text{prevMove} \rangle$  with smallest  $f$  from  $O$
- 8:   **if**  $\text{curr} \in Visited$  **then**
- 9:     **continue**
- 10:     $Visited \leftarrow Visited \cup \{\text{curr}\}$
- 11:    **if**  $\text{curr} = g$  **then**
- 12:     **return** RECONSTRUCTPATH( $CameFrom, g$ )
- 13:    **for** each  $(\Delta x, \Delta y) \in \text{AllowedMoves}$  **do**
- 14:     **nbr**  $\leftarrow \text{curr} + (\Delta x, \Delta y)$
- 15:     **if**  $\text{nbr}$  inside  $G$  **and**  $G(\text{nbr}) = 0$  **and**  $\text{nbr} \notin Visited$  **then**
- 16:        $c \leftarrow \begin{cases} \sqrt{2}, & |\Delta x| = |\Delta y| = 1 \\ 1, & \text{otherwise} \end{cases}$
- 17:        $tent \leftarrow gCost(\text{curr}) + c$
- 18:       **if**  $tent < gCost(\text{nbr})$  **then**
- 19:          $gCost(\text{nbr}) \leftarrow tent$
- 20:          $h \leftarrow \text{COMBH}(\text{nbr}, g, G, \alpha, \beta, r)$
- 21:          $f' \leftarrow tent + h$
- 22:         Push  $\langle f', \text{nbr}, (\Delta x, \Delta y) \rangle$  into  $O$
- 23:          $CameFrom[\text{nbr}] \leftarrow \text{curr}$
- 24:     **return** FAILURE  $\triangleright$  no path found
- 25: **function** COMBH( $n, g, G, \alpha, \beta, r$ )
- 26:     $h_1 \leftarrow |x(n) - x(g)| + |y(n) - y(g)|$   $\triangleright$  Manhattan
- 27:     $h_\infty \leftarrow \max(|x(n) - x(g)|, |y(n) - y(g)|)$   $\triangleright$  Chebyshev
- 28:     $S \leftarrow \text{DYNAMICSAFETYCOST}(n, G, r)$
- 29:    **return**  $\alpha h_1 + (1 - \alpha) h_\infty + \beta S$
- 30: **function** DYNAMICSAFETYCOST( $n, G, r$ )
- 31:     $S \leftarrow 0$ ;  $(x, y) \leftarrow n$
- 32:    **for** each  $(\delta x, \delta y)$  with  $\max(|\delta x|, |\delta y|) \leq r$  **and**  $(\delta x, \delta y) \neq (0, 0)$  **do**
- 33:        $(u, v) \leftarrow (x + \delta x, y + \delta y)$
- 34:       **if**  $(u, v)$  inside  $G$  **and**  $G(u, v) = 1$  **then**  $\triangleright 1 = \text{obstacle}$
- 35:          $d \leftarrow \max(|\delta x|, |\delta y|)$
- 36:          $S \leftarrow S + \frac{1}{d + \varepsilon}$   $\triangleright \varepsilon > 0$  small
- 37:    **return**  $S$

---

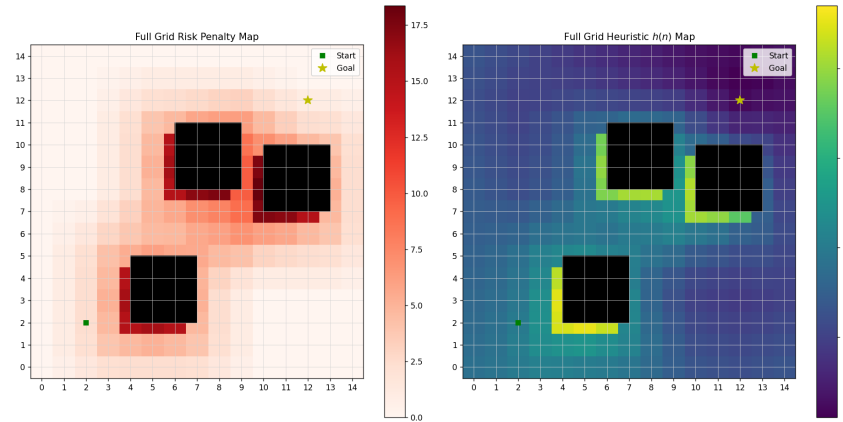


Fig. 1: Visualization of the heuristic formulation. **Left:** Risk penalty map showing the influence of nearby obstacles using the weighted proximity-based term. **Right:** Full heuristic map  $h(n)$  combining the Manhattan distance  $h_1(n, g)$ , Chebyshev distance  $h_\infty(n, g)$ , and obstacle proximity penalties. Black squares denote obstacles; the green square is the start node and the yellow star is the goal.

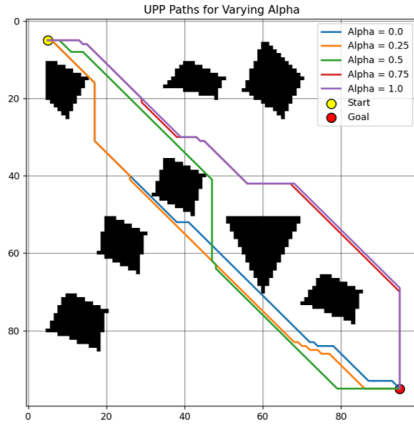


Fig. 2: Depicts the effect of variable alpha

Variable Beta	Average of Minimum Distance from Obstacles (m)	Minimum Distance from Obstacles (m)
0.25	6.67	1
0.5	8.57	4.24
1	9.89	6
5	11.3	6

TABLE II: Metrics for comparison of variable beta

### B. Variation of Beta

Table 2 and Fig. 3 represent the effect of  $\beta$  on the path in metrics and visualization, respectively. It can be seen that as beta increases, the average minimum distance from obstacles increases.  $\beta$  is a scaling factor for dynamic safety cost; the higher the  $\beta$ , the higher the safety. It can be adjusted according to the needs of the user. The minimum of ( average minimum average distance) and (minimum distance) are with  $\beta = 0.25$ , i.e., 6.67 m and 1m respectively. The maximum are with  $\beta = 5$ , i.e., 11.3 m and 6m respectively.

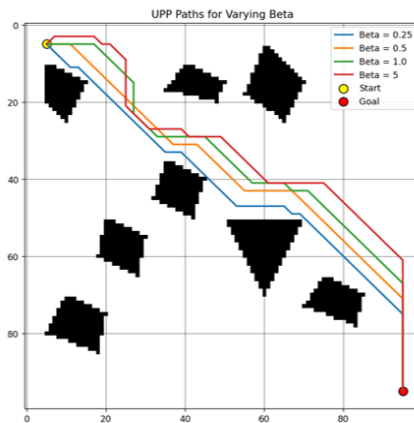
### C. Variation of Radius

Variable Radius	Average of Minimum Distance from Obstacles (m)	Planning Time (ms)
1	6.92	43.32
2	7.66	52.75
3	8.25	87.80
5	8.81	154.20
10	10.89	457.02
50	16.40	6697.65

TABLE III: Metrics for comparison of variable Radius

Table 3 and Fig. 4 represent the effect of R on the path in metrics and visualization, respectively. The radius R depicts how the size of the local region is used in safety cost evaluation for planning. It is based on the vision capabilities of the robot and how far, within a radius R, a robot can

Fig. 3: Depicts the effect of variable beta



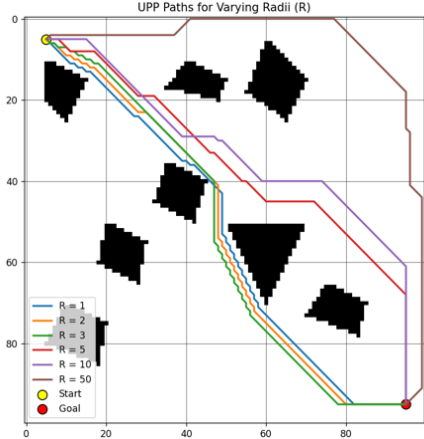


Fig. 4: Depicts the effect of variable Radius

see. It estimates obstacle proximity from nodes. As can be seen in Table 3, with increasing radius from  $R=1$ , the average of minimum distance and planning time, 6.92 m and 43.32 ms, increases to 16.4m and 6697.5 ms with  $R=50$ . This is because as the radius increases, it considers more nodes in computation and safety, leading to safe paths with an increased average of minimum distances and planning time. There is a trade-off between the amount of safety and computational complexity that can be adjusted as needed.

#### D. Comparison of Algorithms

The comparison of UPP is performed with various algorithms to give insights, which include traditional algorithms A\*, Voronoi Planner, RRT, and safe-optimal algorithms like Optimized-A\* [24], CBF-RRT [25], and SDF-A\* [26]. These algorithms have been compared in 5 scenarios of different configurations for 1000 iterations each for random start and goal , mean over all iterations is depicted in the table. These simulations have been performed with constant parameters. We chose  $\alpha = 0.5$  because it balances Manhattan and Chebyshev components (minimal turning angle),  $\beta = 0.5$  ensures moderate obstacle clearance without excessive path inflation, and  $R = 8$  provides sufficient safety lookahead with manageable planning time.

Algorithm	Metrics				
	Success Rate (in %)	Planning Time (ms)	Path Cost (m)	Total Turning Angle (°)	Minimum Distance from Obstacles (m)
CBF*-RRT	94.68	22314.04	87.46	2308.73	4.61
Optimized A*	100	44.93	72.58	175.68	4.82
RRT	100	4.7	82.49	641.76	4.05
SDF-A*	100	531.87	65.49	459.39	5.32
Traditional A*	100	4.46	62.2	173.12	4.79
UPP (Ours)	100	73.79	62.92	190.1	5.8
Voronoi	56.93	5.12	86.98	247.63	5.47

TABLE IV: Comparison of planning algorithms in different scenarios

Table 4 represents the comparison of various algorithms in various scenarios over a total of 5000 iterations. All planners achieve a 100% success rate except CBF\*-RRT and Voronoi. The Voronoi planner's failures were primarily

observed in scenarios with narrow corridors, where a valid Voronoi path could not be generated. UPP produces an average path cost of 62.92 m, which is only 1.15% higher than Traditional A\* while offering an average minimum obstacle clearance of 5.8 m — 0.33 m greater than Voronoi — with perfect planning efficiency. Compared to Voronoi, UPP delivers a 38.2% lower path cost while maintaining higher safety. In terms of smoothness, UPP performs slightly worse than Traditional A\* and Optimized A\*, yet still achieves a balanced compromise between safety and optimality better than most other algorithms. Its planning time is modestly higher than Voronoi, Traditional A\*, and Optimized A\* due to targeted exploration in designated safety regions. Importantly, UPP's heuristic parameters allow the trade-off between optimality and safety to be flexibly tuned to meet specific task requirements.

## V. EXPERIMENTAL RESULTS

In this section, we present the results of the experiments of the proposed method on a hardware test-bench of a TurtleBot robot. The TurtleBot was equipped with a LiDAR sensor that was used for Simultaneous Localization and Mapping (SLAM), and ROS2-humble was used as the interface. Mapping was done using the cartographer package inside the lab, forming an area with few obstacles. UPP was integrated as a global planner in the Nav2 package in Turtlebot, and DWA was used as a local planner for obstacle avoidance. The parameters were the same as those used in the simulation except  $\beta = 2$  for increased safety. The task of the robot was to plan a safe path in an obstacle-rich environment while ensuring near-optimality of the path obtained. We compared UPP against the default Nav2 global planner used in TurtleBot because it is the standard setup in TurtleBot and widely adopted in ROS2 navigation benchmarks, ensuring both fairness and practical relevance. As seen in Table 5,

TABLE V: Average performance comparison of Nav2 and UPP over 5 experiments.

	PathCost	MinDist	TurnCost	TimeToGoal
Nav2	3.532	<b>0.108</b>	8.96	32.732
UPP (Ours)	<b>2.942</b>	0.081	<b>5.461</b>	<b>28.126</b>

UPP shows improvements in path cost, turning cost, and time-to-goal compared to the default Nav2 planner. While Nav2 maintains a slightly higher minimum clearance, UPP provides a good balance between efficiency and safety in navigation tasks. While hardware validation is limited to Nav2, our simulations (Sec. IV) provide broader comparisons with other planners to indicate UPP's balanced performance. A demonstration video and code for UPP as a Nav2 planner plugin are included in the supplementary material for this paper.

## VI. CONCLUSION

In this paper, we have proposed a Unified Path Planner, a unified framework for optimality and safety in planning, compared to other algorithms that mainly deal with either

optimality or safety. The flexibility in UPP allows tuning of the optimality and safety trade-off depending on the computational power available. We have compared this algorithm with various traditional and suboptimal safe algorithms in extensive simulations in various environments in this paper. UPP was able to perform, on average, better in terms of safety, while accruing a path cost close to that of the optimal algorithms. However, in sparse scenarios, Optimized A\* and other algorithms were able to better balance safety and optimality. Future research will focus on extending the UPP framework to include perception uncertainty and to handle dynamic obstacles by incorporating their predicted trajectories into the safety cost calculation.

## REFERENCES

- [1] B. Paden, M. Cap, S. Z. Yong, D. Yershov, and E. Frazzoli, “A survey of motion planning and control techniques for self-driving urban vehicles,” *IEEE Transactions on Intelligent Vehicles*, vol. 1, no. 1, p. 33–55, Mar. 2016. [Online]. Available: <http://dx.doi.org/10.1109/TIV.2016.2578706>
- [2] C. Li, J. Wang, X. Wang, and Y. Zhang, “A model based path planning algorithm for self-driving cars in dynamic environment,” in *2015 Chinese Automation Congress (CAC)*. IEEE, Nov. 2015, p. 1123–1128. [Online]. Available: <http://dx.doi.org/10.1109/CAC.2015.7382666>
- [3] U. Lee, S. Yoon, H. Shim, P. Vasseur, and C. Demonceaux, “Local path planning in a complex environment for self-driving car,” in *The 4th Annual IEEE International Conference on Cyber Technology in Automation, Control and Intelligent*. IEEE, June 2014, p. 445–450. [Online]. Available: <http://dx.doi.org/10.1109/CYBER.2014.6917505>
- [4] S. Bortoff, “Path planning for uavs,” in *Proceedings of the 2000 American Control Conference. ACC (IEEE Cat. No.00CH36334)*. IEEE, 2000, p. 364–368 vol.1. [Online]. Available: <http://dx.doi.org/10.1109/ACC.2000.878915>
- [5] Y. Dai, C. Xiang, Y. Zhang, Y. Jiang, W. Qu, and Q. Zhang, “A review of spatial robotic arm trajectory planning,” *Aerospace*, vol. 9, no. 7, p. 361, July 2022. [Online]. Available: <http://dx.doi.org/10.3390/aerospace9070361>
- [6] M. H. Korayem, H. R. Nohooji, and A. Nikoobin, “Path planning of mobile elastic robotic arms by indirect approach of optimal control,” *International Journal of Advanced Robotic Systems*, vol. 8, no. 1, Jan. 2011. [Online]. Available: <http://dx.doi.org/10.5772/10524>
- [7] B. K. Kim and K. G. Shin, “Minimum-time path planning for robot arms and their dynamics,” *IEEE Transactions on Systems, Man, and Cybernetics*, vol. SMC-15, no. 2, p. 213–223, Mar. 1985. [Online]. Available: <http://dx.doi.org/10.1109/TSMC.1985.6313351>
- [8] S. Klanke, D. Lebedev, R. Haschke, J. Steil, and H. Ritter, “Dynamic path planning for a 7-dof robot arm,” in *2006 IEEE/RSJ International Conference on Intelligent Robots and Systems*. IEEE, Oct. 2006, p. 3879–3884. [Online]. Available: <http://dx.doi.org/10.1109/IROS.2006.281798>
- [9] J. Hvezda, T. Rybecky, M. Kulich, and L. Preucil, “Context-aware route planning for automated warehouses,” in *2018 21st International Conference on Intelligent Transportation Systems (ITSC)*. IEEE, Nov. 2018, p. 2955–2960. [Online]. Available: <http://dx.doi.org/10.1109/ITSC.2018.8569712>
- [10] K. C. T. Vivaldini, J. P. M. Galdames, T. S. Bueno, R. C. Araujo, R. M. Sobral, M. Becker, and G. A. P. Caurin, “Robotic forklifts for intelligent warehouses: Routing, path planning, and auto-localization,” in *2010 IEEE International Conference on Industrial Technology*. IEEE, Mar. 2010, p. 1463–1468. [Online]. Available: <http://dx.doi.org/10.1109/ICIT.2010.5472487>
- [11] P. Hart, N. Nilsson, and B. Raphael, “A formal basis for the heuristic determination of minimum cost paths,” *IEEE Transactions on Systems Science and Cybernetics*, vol. 4, no. 2, p. 100–107, 1968. [Online]. Available: <http://dx.doi.org/10.1109/TSSC.1968.300136>
- [12] C. Warren, “Fast path planning using modified a\* method,” in *[1993] Proceedings IEEE International Conference on Robotics and Automation*. IEEE Comput. Soc. Press, p. 662–667. [Online]. Available: <http://dx.doi.org/10.1109/ROBOT.1993.291883>
- [13] A. Nash and S. Koenig, “Any-angle path planning,” *AI Magazine*, vol. 34, no. 4, p. 85–107, Dec. 2013. [Online]. Available: <http://dx.doi.org/10.1609/aimag.v34i4.2512>
- [14] A. Stentz, “Optimal and efficient path planning for partially-known environments,” in *Proceedings of the 1994 IEEE International Conference on Robotics and Automation*, ser. ROBOT-94. IEEE Comput. Soc. Press, p. 3310–3317. [Online]. Available: <http://dx.doi.org/10.1109/ROBOT.1994.351061>
- [15] I. Noreen, A. Khan, and Z. Habib, “Optimal path planning using rrt\* based approaches: A survey and future directions,” *International Journal of Advanced Computer Science and Applications*, vol. 7, no. 11, 2016. [Online]. Available: <http://dx.doi.org/10.14569/IJACSA.2016.071114>
- [16] J. Nasir, F. Islam, U. Malik, Y. Ayaz, O. Hasan, M. Khan, and M. S. Muhammad, “Rrt\*-smart: A rapid convergence implementation of rrt\*,” *International Journal of Advanced Robotic Systems*, vol. 10, no. 7, Jan. 2013. [Online]. Available: <http://dx.doi.org/10.5772/56718>
- [17] Z. Wu, Z. Meng, W. Zhao, and Z. Wu, “Fast-rrt: A rrt-based optimal path finding method,” *Applied Sciences*, vol. 11, no. 24, p. 11777, Dec. 2021. [Online]. Available: <http://dx.doi.org/10.3390/app112411777>
- [18] S. M. LaValle, *Planning Algorithms*. Cambridge, U.K.: Cambridge University Press, 2006, available at <http://planning.cs.uiuc.edu/>.
- [19] H. Jafarzadeh and C. H. Fleming, “An exact geometry-based algorithm for path planning,” *International Journal of Applied Mathematics and Computer Science*, vol. 28, no. 3, p. 493–504, Sept. 2018. [Online]. Available: <http://dx.doi.org/10.2478/amcs-2018-0038>
- [20] B. B. K. Ayawli, X. Mei, M. Shen, A. Y. Appiah, and F. Kyeremeh, “Mobile robot path planning in dynamic environment using voronoi diagram and computation geometry technique,” *IEEE Access*, vol. 7, p. 86026–86040, 2019. [Online]. Available: <http://dx.doi.org/10.1109/ACCESS.2019.2925623>
- [21] Y. Hwang and N. Ahuja, “A potential field approach to path planning,” *IEEE Transactions on Robotics and Automation*, vol. 8, no. 1, p. 23–32, 1992. [Online]. Available: <http://dx.doi.org/10.1109/70.127236>
- [22] S. M. H. Rostami, A. K. Sangaiah, J. Wang, and X. Liu, “Obstacle avoidance of mobile robots using modified artificial potential field algorithm,” *EURASIP Journal on Wireless Communications and Networking*, vol. 2019, no. 1, Mar. 2019. [Online]. Available: <http://dx.doi.org/10.1186/s13638-019-1396-2>
- [23] A. Azzabi and K. Nouri, “An advanced potential field method proposed for mobile robot path planning,” *Transactions of the Institute of Measurement and Control*, vol. 41, no. 11, p. 3132–3144, Jan. 2019. [Online]. Available: <http://dx.doi.org/10.1177/0142331218824393>
- [24] L. Chu, Y. Wang, S. Li, Z. Guo, W. Du, J. Li, and Z. Jiang, “Intelligent vehicle path planning based on optimized a\* algorithm,” *Sensors*, vol. 24, no. 10, p. 3149, May 2024. [Online]. Available: <http://dx.doi.org/10.3390/s24103149>
- [25] A. Manjunath and Q. Nguyen, “Safe and robust motion planning for dynamic robotics via control barrier functions,” in *2021 60th IEEE Conference on Decision and Control (CDC)*. IEEE, Dec. 2021, p. 2122–2128. [Online]. Available: <http://dx.doi.org/10.1109/CDC45484.2021.9682803>
- [26] H. Wang, Y. Lin, W. Zhang, W. Ye, M. Zhang, and X. Dong, “Safe autonomous exploration and adaptive path planning strategy using signed distance field,” *IEEE Access*, vol. 11, p. 144663–144675, 2023. [Online]. Available: <http://dx.doi.org/10.1109/ACCESS.2023.3344218>
- [27] S. J. Russell and P. Norvig, *Artificial Intelligence: A Modern Approach (4th Edition)*. Pearson, 2020. [Online]. Available: <http://aima.cs.berkeley.edu/>
- [28] A. Archetti, M. Cannici, and M. Matteucci, *Neural Weighted A\*: Learning Graph Costs and Heuristics with Differentiable Anytime A\**. Springer International Publishing, 2022, p. 596–610. [Online]. Available: [http://dx.doi.org/10.1007/978-3-030-95467-3\\_43](http://dx.doi.org/10.1007/978-3-030-95467-3_43)
- [29] R. Valenzano, S. Arfaee, J. Thayer, R. Stern, and N. Sturtevant, “Using alternative suboptimality bounds in heuristic search,” 06 2013.